

Laser Damage Threshold Measurements of Micro-Structure Based High Reflectors

Douglas S. Hobbs*

TelAztec LLC, 15 A Street, Burlington, Massachusetts 01803 USA

ABSTRACT

In 2007, the pulsed laser induced damage threshold (LIDT) of anti-reflecting (AR) microstructures built in fused silica and glass was shown to be up to three times greater than the LIDT of single-layer thin-film AR coatings, and at least five times greater than multiple-layer thin-film AR coatings. This result suggested that microstructure-based wavelength selective mirrors might also exhibit high LIDT. Efficient light reflection over a narrow spectral range can be produced by an array of sub-wavelength sized surface relief microstructures built in a waveguide configuration. Such surface structure resonant (SSR) filters typically achieve a reflectivity exceeding 99% over a 1-10nm range about the filter center wavelength, making SSR filters useful as laser high reflectors (HR). SSR laser mirrors consist of microstructures that are first etched in the surface of fused silica and borosilicate glass windows and subsequently coated with a thin layer of a non-absorbing high refractive index dielectric material such as tantalum pent-oxide or zinc sulfide. Results of an initial investigation into the LIDT of single layer SSR laser mirrors operating at 532nm, 1064nm and 1573nm are described along with data from SEM analysis of the microstructures, and spectral reflection measurements. None of the twelve samples tested exhibited damage thresholds above 3 J/cm² when illuminated at the resonant wavelength, indicating that the simple single layer, first order design will need further development to be suitable for high power laser applications. Samples of SSR high reflectors entered in the Thin Film Damage Competition also exhibited low damage thresholds of less than 1 J/cm² for the ZnS coated SSR, and just over 4 J/cm² for the Ta₂O₅ coated SSR.

Keywords: laser mirrors, microstructures, laser induced damage threshold, LIDT, rejection filters, waveguide resonant gratings, dielectric mirrors, thin-film coatings

1. INTRODUCTION

The very high reflectivity mirrors needed for many important laser applications such as the laser fusion project, laser communications, industrial laser cutting systems, and laser radar and weapon systems, all require increased laser damage resistance as the operational energy continues to rise. Over the course of many years, multiple-layer thin-film interference coatings have been developed to a level where high reflectivity and high damage resistance is achieved using several types of dielectric materials and many deposition methods. Current trends favor the high-low refractive index combination of hafnium or tantalum oxide (HfO₂ or Ta₂O₅) and silicon dioxide (SiO₂) coatings deposited by e-beam evaporation techniques. To produce a near infrared laser high reflector with more than 99% reflectance calls for a large number of thin-film layers (at least 20 and typically more than 30) to be deposited with great precision and with careful consideration of the material stresses and initial substrate conditions^[1]. Such processing complexity yields high costs and may limit the achievable performance for some high power applications. An alternative high reflector (HR) technology based on surface relief microstructures has the potential to achieve performance levels similar to thin-film HR stacks using a low cost fabrication process requiring just one or two material depositions. The potential for simple HR microstructures to exhibit high pulsed laser induced damage thresholds (LIDT) was investigated in this initial study.

2. MICROSTRUCTURE BASED WAVELENGTH SELECTIVE MIRRORS

Examples of microstructures that produce efficient light reflection are found throughout the natural world^[2]. Brilliant blue and violet light reflections are created through constructive interference from the multi-faceted or stepped microstructures found on the wings of several butterfly species^[3,4]. Artificial butterfly-wing microstructures are being developed by Dr. James Cowan (one of TelAztec's founders now retired)^[5,6]. Two types of "Aztec" microstructure reflectors are shown in Figure 1, with the top row giving scanning electron micrographs (SEM) images viewed from overhead, and the bottom row giving a diagram of the structures in profile. The reflected color is given by the step height (h) and the incident medium refractive index (n₀). For the symmetric Aztec Color Reflector, the reflected light

* Correspondence: DSHobbs@telaztec.com, Voice: 781-229-9905, Fax: 781-229-2195 www.telaztec.com

propagates in the specular direction which is useful for on-axis systems such as lasers, whereas the asymmetric Aztec Color Diffusers are designed to separate and diffuse the color reflection from any specularly reflected light making them useful as background light in displays or for creating holographic images. Figure 2 shows the measured normal incidence reflection from Aztec Color Reflectors replicated into a plastic sheet and subsequently coated with aluminum to enhance the reflectivity of each step. The step height was varied in three separate areas to produce different colors. Each of the textures contained microstructures with 5-steps arranged in a honeycomb grid as shown in the SEM image inset. The reflectivity (relative to aluminum) varies from 20-25% with a half maximum bandwidth of over 70nm.

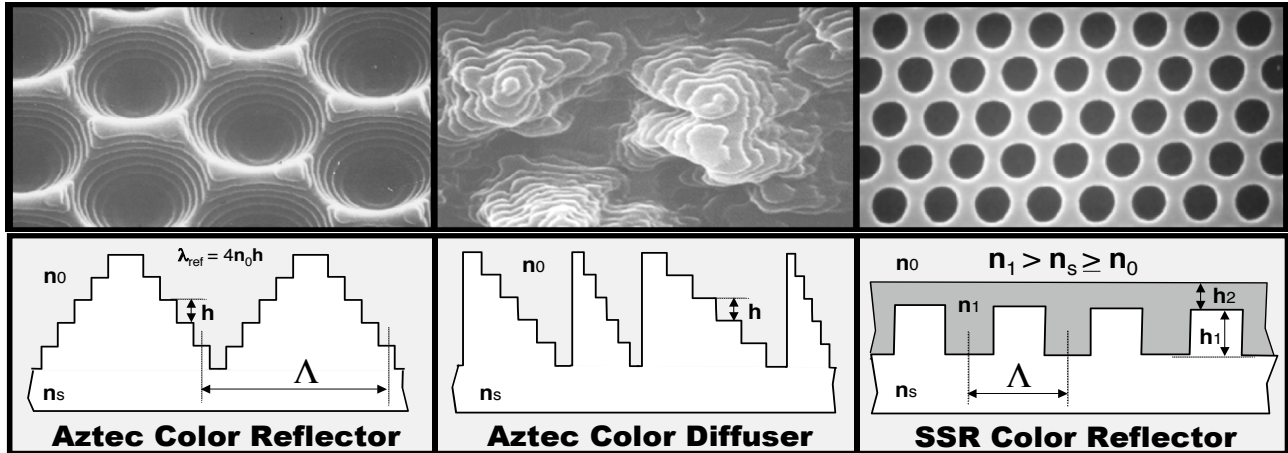


Figure 1. SEM images (top row) and cross sectional diagrams (bottom row) of Aztec and SSR wavelength selective mirrors.

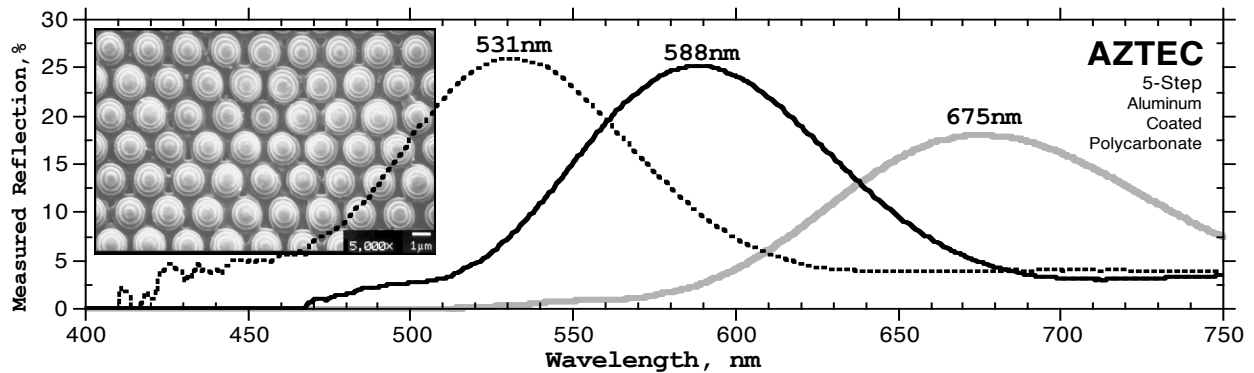


Figure 2. SEM image (inset) and measured normal incidence reflection of 5-step Aztec color reflectors with 3 step heights.

Aztec structures are quite difficult to fabricate in durable substrates such as glass and fused silica, and because the efficiency of the reflection depends on the reflectivity of each individual step, the number of steps needed to produce greater than 99% reflectivity becomes impractically large. To achieve high efficiency reflection, an alternative design based on microstructures in a waveguide configuration can be exploited. On the right in Figure 1 is an image and cross sectional diagram of a regular array holes that have been etched in a glass substrate and subsequently coated with a layer of material with a refractive index (n_1) that is larger than the glass refractive index (n_s) and the incident medium refractive index (n_0). The microstructures cause incident light within a particular wavelength range to be diffracted into the waveguide region formed by the high refractive index coating. As the diffracted wave propagates within the waveguide a strong resonance can be accumulated over a narrow wavelength range through reflection from the individual microstructures in the array. This surface structure resonance (SSR) concept has been referred to as “photonic bandgaps” in the literature^[7-23].

Figure 3 shows the measured reflection of visible light from an SSR color reflector created by coating microstructures etched in borofloat glass with a conformal layer of zinc sulfide (ZnS). Overhead and elevation views of the coated microstructures are also shown in the figure. A blue reflection approaching 100% at 451 nanometer (nm) is observed, with a full width half maximum (FWHM) bandwidth of about 50nm. Such high performance attained with just a single

material coating suggests that the SSR concept could be adapted to produce laser mirrors with damage thresholds equivalent to or better than dielectric mirrors created from multiple-layer thin-film interference coatings.

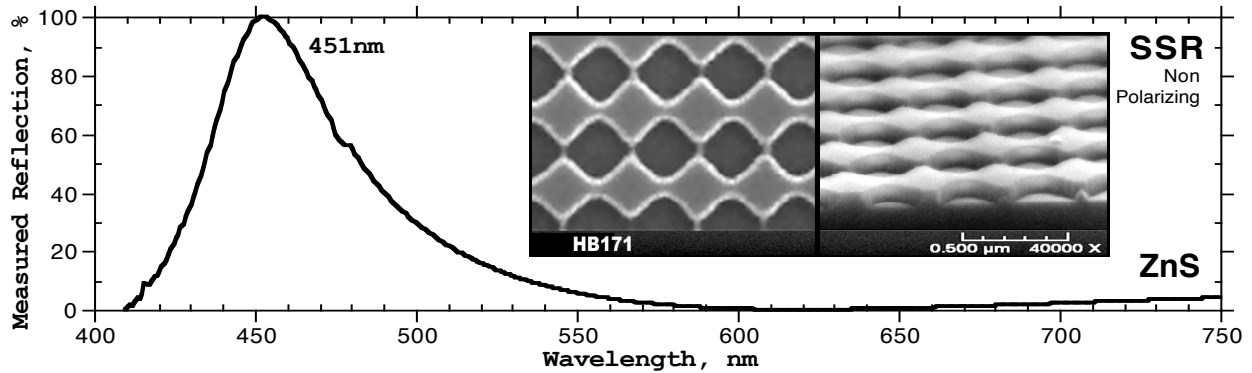


Figure 3. SEM images (inset) and the measured normal incidence reflection of a non-polarizing SSR blue reflector.

Because an SSR mirror interacts with light in a plane transverse to the light propagation direction, the introduction of microstructure asymmetry can produce unique polarization effects. SSR laser cavity mirrors can be built to select for both wavelength and polarization enabling wavelength stabilization and reduced component counts in many high power laser systems. The measured performance of a polarizing SSR laser mirror produced from microstructures etched into a Ta₂O₅ layer coated on a borofloat glass window (inset images), are shown in Figure 4. Separate resonances are observed at 625nm and 675nm in the red for linearly polarized light oriented in orthogonal directions. The p-polarized resonance is over 95% efficient with a 10nm FWHM bandwidth and a peak polarization extinction ratio of over 1000:1.

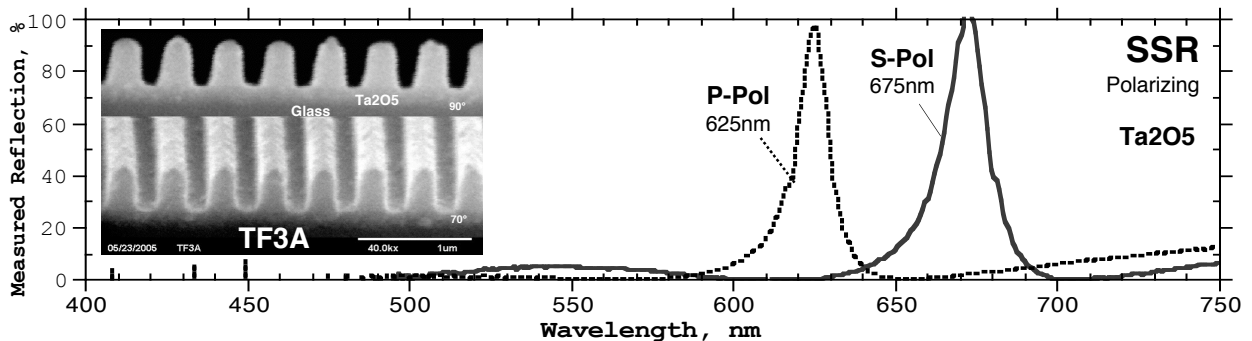


Figure 4. SEM images (inset) and the measured normal incidence reflection of a polarizing SSR laser mirror.

3. SSR LASER MIRROR DESIGN

For this initial damage threshold study of SSR laser mirrors, a simple design was chosen based on microstructures etched in glass and fused silica substrates that are coated with a single layer of high refractive index material. Both ZnS ($n \sim 2.3$) deposited by e-beam evaporation, and Ta₂O₅ ($n \sim 2.05$) deposited by ion assisted deposition (IAD), were readily available from Omega Optical of Vermont. These material choices were input to computer modeling software to predict the reflectivity of the SSR mirrors configured to resonate at 532nm, 1064nm, and 1538nm – laser wavelengths for which calibrated pulsed laser damage measurements can be made using the services of Quantel USA (formerly Big Sky Laser) of Montana. Figure 5 plots the modeling results for the three design wavelengths where the dashed curves show ZnS coated microstructures and the solid curves represent Ta₂O₅ coated microstructures. The models predict little difference in performance when using borofloat glass or fused silica. The resonant wavelength is shifted from 532nm to 1064nm to 1538nm simply by changing the microstructure spacing, or pitch, and by increasing the thickness of the ZnS or Ta₂O₅ layer. The diagrams inset in the upper right in each plot represent the symmetric, non-polarizing SSR configuration model input to the software simulation. Note that the higher refractive index of ZnS yields slightly larger bandwidth performance than the Ta₂O₅ coated SSRs, and that the bandwidth increases for longer wavelength resonator configurations.

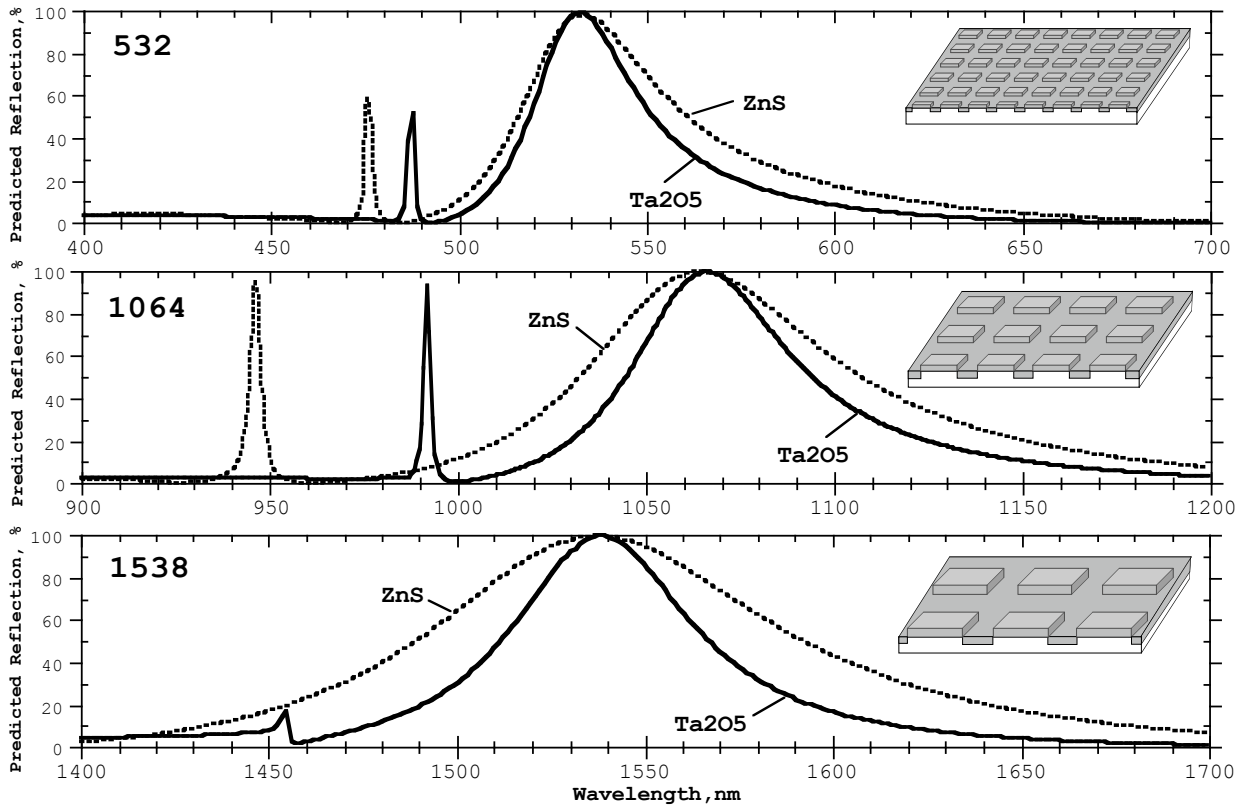


Figure 5: Predicted reflection of SSR mirrors at 532, 1064, and 1538nm for both ZnS and Ta2O5 coatings.

For applications requiring wider bandwidth reflection or a greater tolerance for the illumination angle of incidence, an SSR mirror can be modified in a variety of ways. With single layer SSR reflectors, the depth of the microstructures and the thickness of the high refractive index coating can be increased to effectively split the resonance producing a dual-peaked performance. In this manner the 95% bandwidth of the Figure 5 designs can be increased from just a few nanometers to as much as 15nm. A more effective method for increasing the 95% bandwidth up to the 100nm range is to deposit additional material layers. Figure 6 shows the predicted reflection of the same microstructures modeled in the top chart of Figure 5 coated with additional layers of silicon oxide (SiO₂) and ZnS. Each of the three material layers is deposited in a manner that conforms to the microstructure surface, effectively replicating the microstructures in each layer. A cross section of the modeled structure is shown at the top right of the plot.

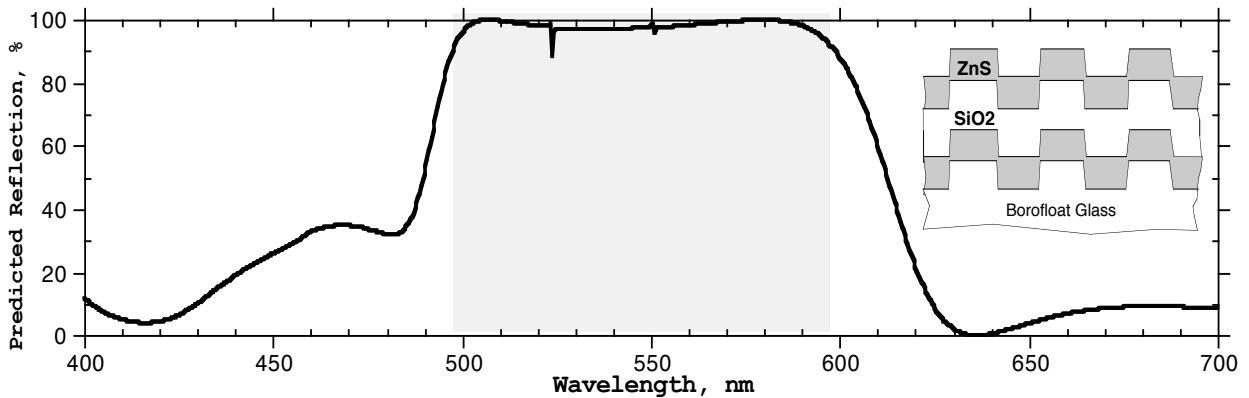


Figure 6: Predicted reflection of a three layer SSR mirror at 532nm with a 95% bandwidth of 100nm.

4. FABRICATION

The microstructures that define an SSR laser mirror are generated in a two-stage process. First lithography is used to record the microstructure pattern in a sacrificial mask material. Second the mask is employed in a conventional dry etching process that transfers the mask pattern into the substrate, or into a pre-deposited material layer. Figure 7 shows a process flow diagram used to produce the SSR mirrors for this study. Schott Borofloat 33 glass windows and custom polished fused silica windows are first cleaned in an acid bath (step 1) before depositing a photosensitive polymer layer by a conventional spin coating method (step 2 using an AZ1500 series photoresist). Next, TelAztec uses its non-contact, maskless, interference lithography tool systems^[24] (images at the top of the step 3 window) to expose a latent image of the SSR texture in the photoresist layer (step 3). The microstructure lithography is completed by a wet development step that delineates the image as a surface relief texture in the photoresist layer (step 4, includes an SEM image of a post array in resist on glass). A reactive ion etching tool (shown in the upper left of the step 5 window) creates a plasma that attacks the exposed surface of the glass removing material by both physical and chemical processes. Another acid clean removes any residual mask material or polymers deposited during the plasma etch process (step 6). Lastly, the SSR mirror is completed by a deposition of the high refractive index layer – typically done in vacuum by an e-beam evaporation method, or by an ion assisted deposition method (step 7).

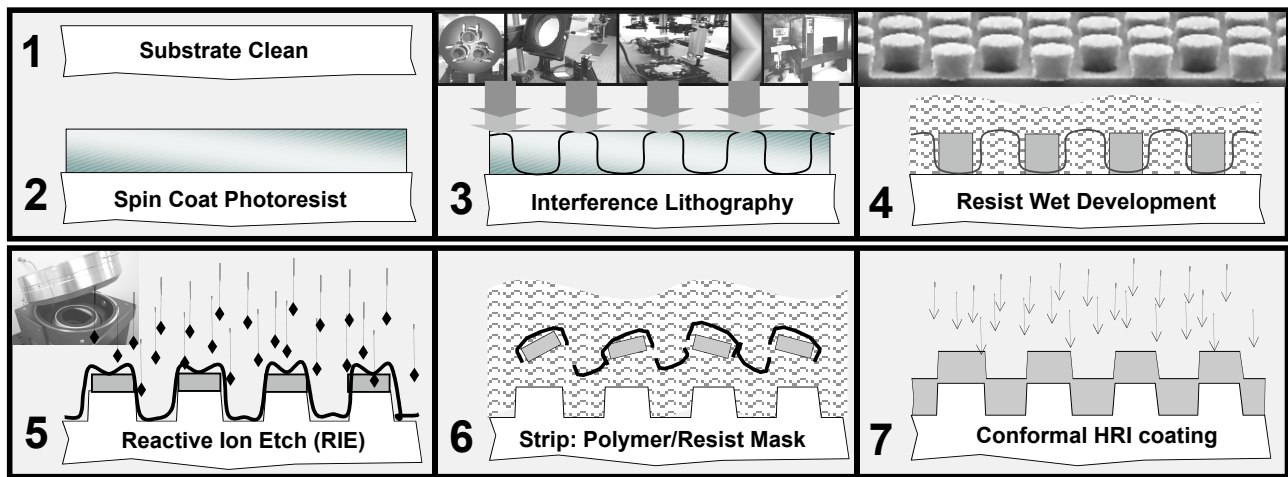


Figure 7. Fabrication process flow diagram for SSR reflectors.

5. CHARACTERIZATION

SSR mirrors are characterized using SEM analysis, and reflectance measurements using both visible and NIR grating-based spectrometers. The visible-NIR spectrometer utilizes a 1024 element silicon detector array and operates over a wavelength range from 400 to 900nm. A recently acquired NIR spectrometer (Ocean Optics Model NIR512) utilizes a 512 element InGaAs detector array and operates over a wavelength range of from 900 to 1700nm. Both spectrometers are coupled to white light sources using multi-mode optical fibers where the light exiting the fibers is collimated by a lens system to produce a probe area of about 3 millimeter (mm) diameter. Light reflected from the probed surface is received by the same fiber for normal incidence reflection measurements, and this reflected light is split into a separate fiber leg that is input to the spectrometer. The reflection from an enhanced aluminum mirror is used as the 100% reference for the visible-NIR system, whereas a protected silver mirror is used for the NIR system reference.

6. SSR MIRROR REFLECTANCE - LASER DAMAGE THRESHOLD MEASUREMENTS

Using the designs and fabrication techniques described in Sections 3 and 4, single layer SSR mirror prototypes were built with high efficiency reflections at 532nm, 1064nm, and 1538nm. After reflectance characterization, the prototypes were submitted for calibrated, NIST traceable, standardized LIDT tests conducted by Jeff Runkel at Quantel USA (Big Sky Laser) in Bozeman Montana. Sixteen thresholds were recorded at three wavelengths using a total of twelve prototypes consisting of two material coatings deposited by two techniques on micro-structured substrates of both Schott Borofloat 33 glass and fused silica. Testing results are given below, organized by laser wavelength.

6.1 LIDT Testing at 532nm

The measured reflection of both polarizing and non-polarizing SSR mirror prototypes designed to resonate at 532nm using ZnS as the high refractive index coating, is shown in Figure 8. (Reflection from the back side of the glass windows was reduced to a low level for the measurement using index matching fluid coupling to a high performance Random AR textured substrate.) The polarizing SSR mirror shown in cross section in the bottom plot of Figure 8, was designed to be bonded with a second substrate using an epoxy. Both ZnS coated prototypes exhibit highly efficient reflection centered at 532nm.

Due to errors in the microstructure fabrication process and adhesion problems in the Ta2O5 coating run, the 532nm SSR mirror prototypes coated with Ta2O5, produced low efficiency reflections peaked at shorter wavelengths. As a result only the two Figure 8 ZnS coated prototypes parts were sent to Quantel for LIDT testing at 532nm. Quantel exposed 110 locations on each window to 10 different fluence levels using a linearly polarized, pulsed laser with a 10ns pulse length and a 0.53mm spot size ($TEM_{00} - 1/e^2$). The pulse repetition rate was 20Hz allowing 200 pulses at each location. The criteria for damage is a permanent surface change as observed by visual inspection through a microscope. The results are shown in Figure 9 where the damage threshold for the laminated, polarizing SSR mirror is just 0.22 J/cm², and the damage threshold for the non-polarizing SSR mirror is 0.93 J/cm². This result is low compared to the 5-10 J/cm² levels typically quoted by mirror vendors.

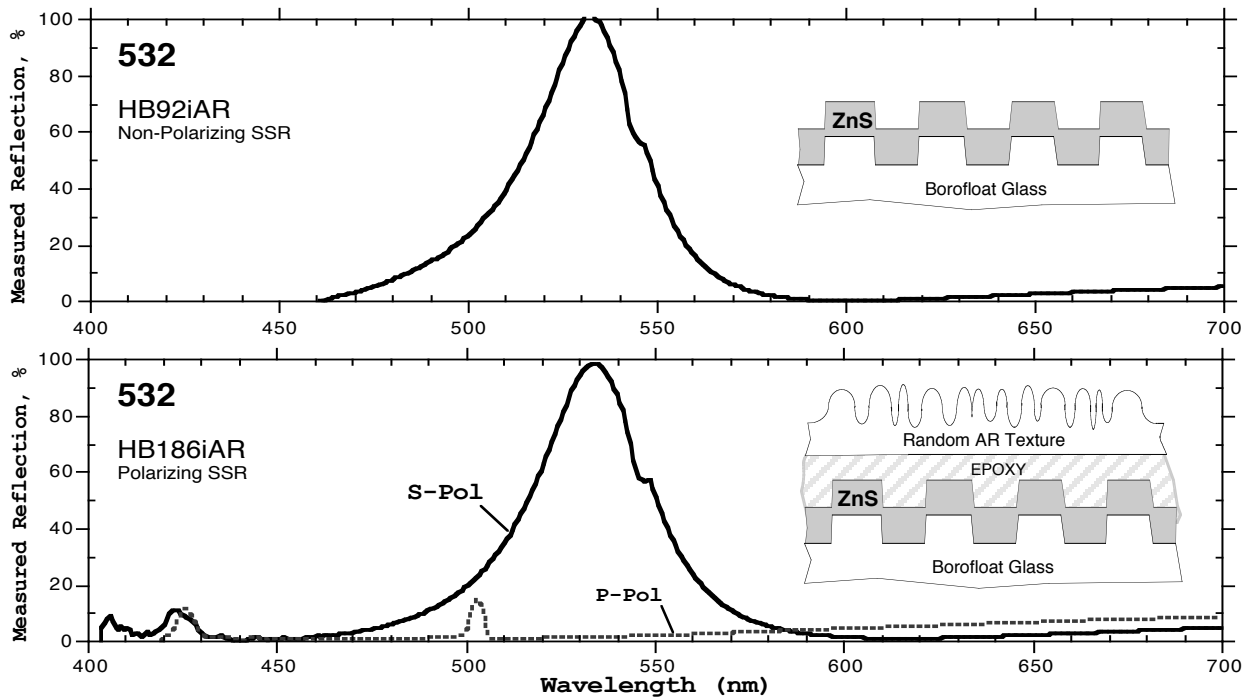


Figure 8: Measured reflection of polarizing and non-polarizing SSR filters submitted for LiDT tests at 532nm.

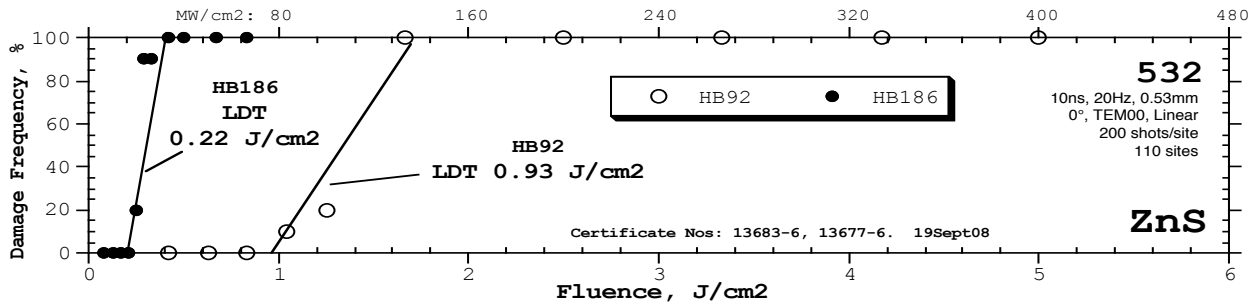


Figure 9: Results of 532nm LIDT testing of the SSR mirror prototypes shown in Figure 8.

6.2 LIDT Testing at 1064nm

To evaluate the LIDT of SSR mirrors at 1064nm, multiple prototypes were fabricated on 1 and 2-inch diameter Schott Borofloat 33 glass windows and on polished fused silica windows. Half the prototypes were coated with ZnS by e-beam evaporation, and the other half were coated with Ta2O5 deposited by ion-assisted deposition. The measured reflection of SSR mirror prototypes designed for 1064nm resonance is shown in Figure 10 along with cross sectional diagrams of the single layer design. (Again the back surface reflections are eliminated by fluid coupling to a high performance Random AR textured substrate during the measurement.) The top plot of Figure 10 shows three SSR samples coated with ZnS, and the bottom plot shows samples coated with Ta2O5. In each plot the dashed curves show the results for the fused silica substrates each resonating at a wavelength longer than the 1064nm target. This is likely due to a variation of the dry etch rates for the fused silica relative to borofloat glass. Prototypes BZ32 and BT20 resonate efficiently at the target wavelength and perform similar to the model prediction. Prototypes BZ14 and BT23 also perform similar to the model prediction with efficient resonances, but are red and blue shifted, respectively, away from the target wavelength. A photograph of all six prototypes is shown on the right with the ZnS coated parts in the upper row and the Ta2O5 coated parts in the lower row.

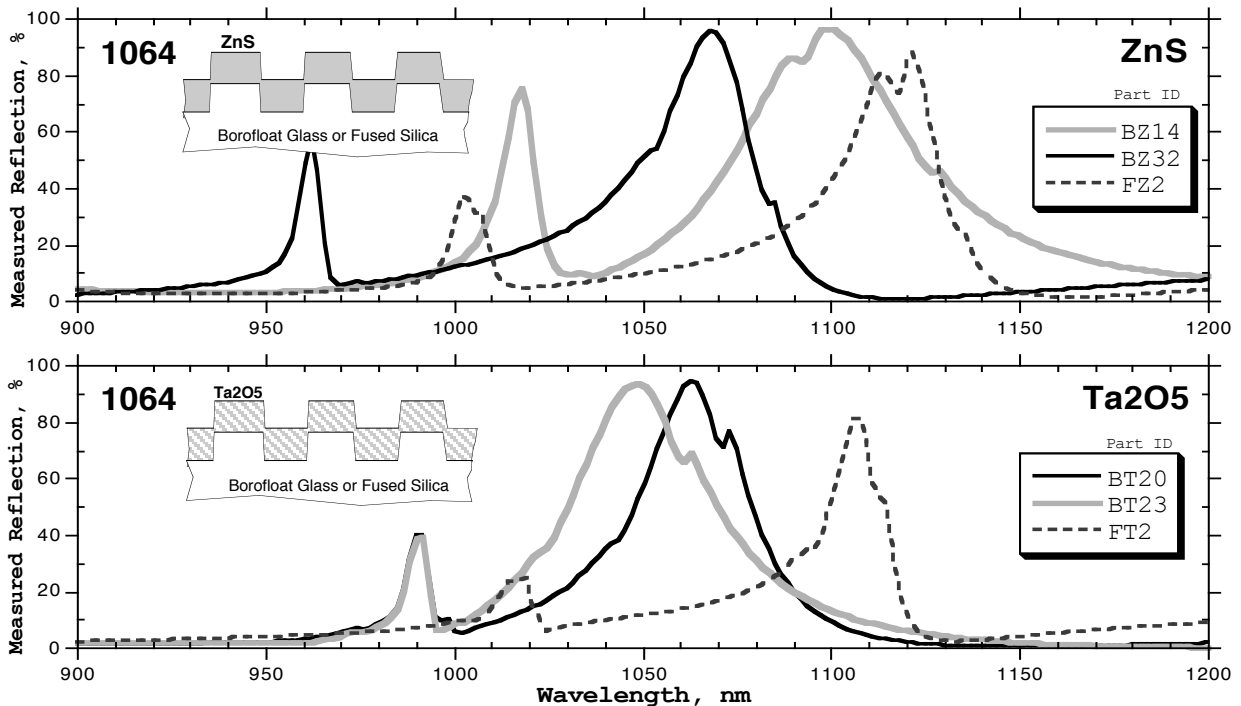
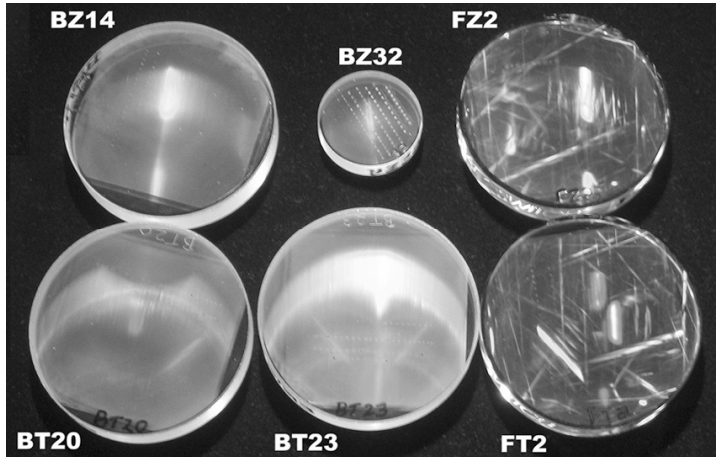


Figure 10: Measured reflection of non-polarizing SSR mirrors submitted for LIDT tests at 1064nm.

The results of the Quantel LIDT testing at 1064nm are shown in Figure 11. Quantel exposed 100 locations on each window to 10 different fluence levels using a linearly polarized, pulsed laser with a 20ns pulse length and a 0.5mm spot size ($TEM_{00} - 1/e^2$). The pulse repetition rate was 20Hz allowing 200 pulses at each location. Again the damage criteria was a permanent surface change as observed by visual inspection through a microscope. The damage thresholds for the non-polarizing SSR mirrors coated with ZnS are just 0.5 J/cm² for BZ32, 1.3 J/cm² for BZ14, and 3.5 J/cm² for the

fused silica part FZ2. The Ta₂O₅ SSR mirror damage thresholds are also low at 0.5 J/cm² for BT20 and BT23, and 2.9 J/cm² for the fused silica part FT2. It was expected that the more dense Ta₂O₅ coating deposited by IAD would exhibit higher damage thresholds than e-beam evaporated ZnS. This was not evident in these low threshold values. It would initially appear that microstructures in fused silica trend toward higher damage thresholds, but because the fused silica SSR mirrors resonate at a longer wavelength the higher thresholds observed may not represent the expected trend. To further investigate the impact of microstructure resonance on the damage threshold, four prototypes fabricated for high reflectivity at 1538nm, were tested for damage threshold at 1064nm. The results given in Figure 12 show damage thresholds about two to three times higher than the thresholds recorded at the resonant wavelength, confirming that the increased electric field intensity within the microstructured-waveguide during resonance leads to greater damage.

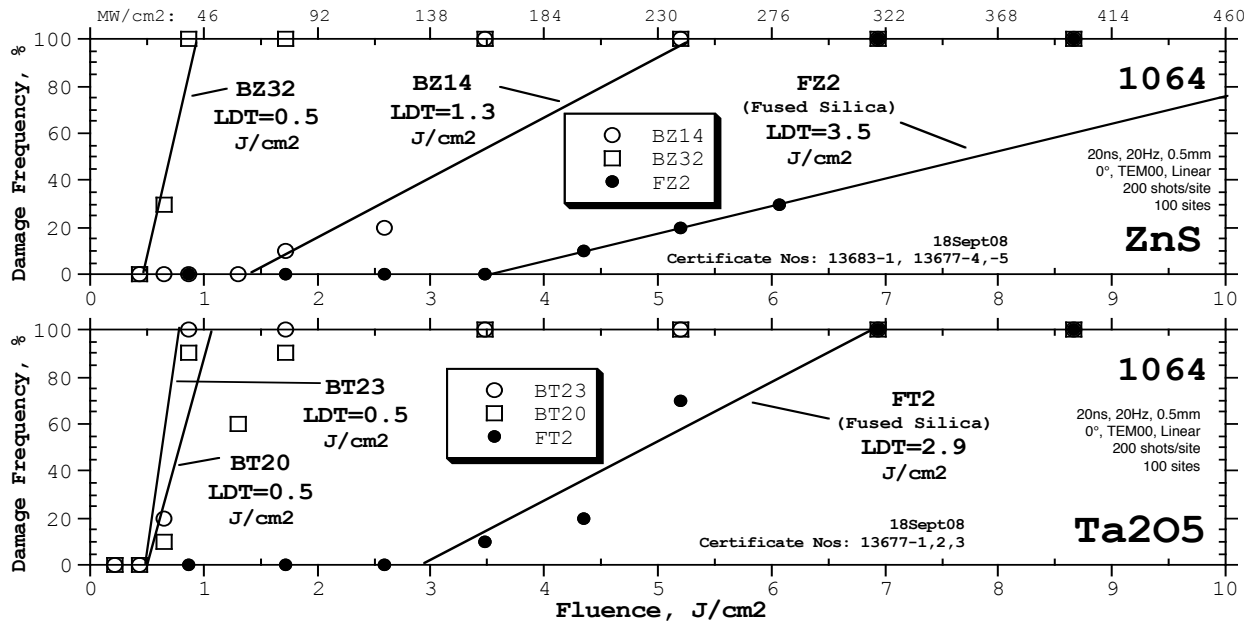


Figure 11: Results of 1064nm LIDT tests of SSR mirrors coated with ZnS (top) and Ta₂O₅ (bottom).

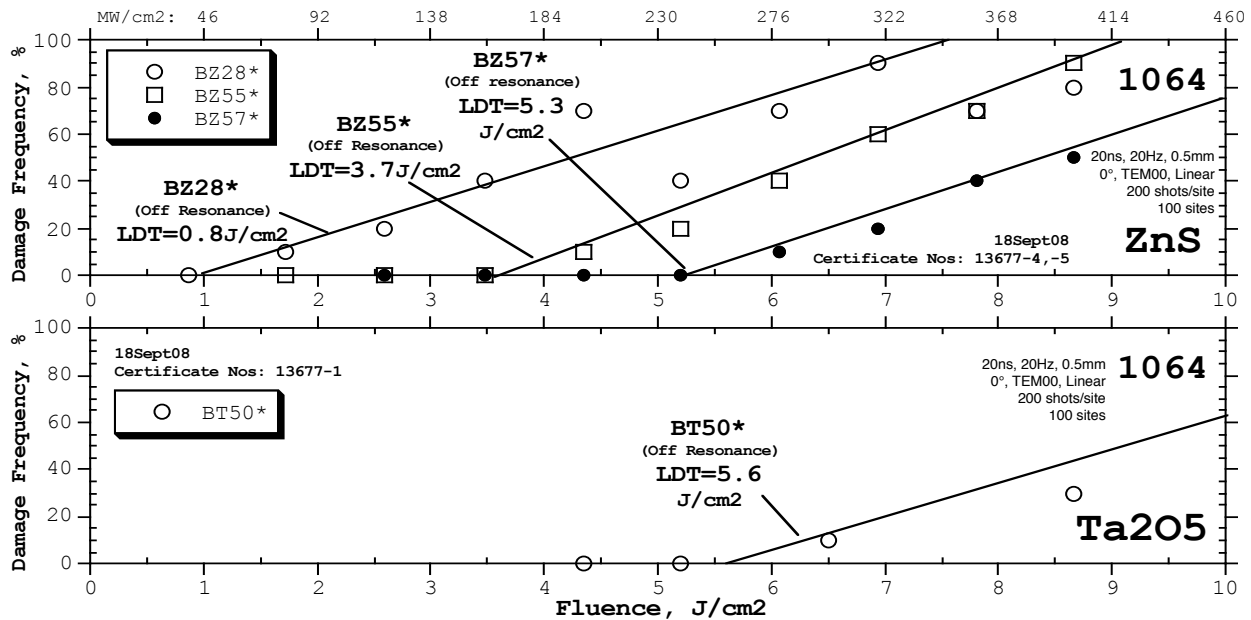


Figure 12: Results of 1064nm LIDT tests of SSR mirrors designed for 1538nm. ZnS (top) and Ta₂O₅ (bottom).

6.3 The 2008 Damage Competition. LIDT Testing at 1064nm

Two polarizing SSR mirror samples were submitted to the Damage Competition. Both mirrors were early prototypes fabricated on Schott Borofloat 33 glass with one sample coated with ZnS and the second sample coated with Ta₂O₅. An estimate of the performance of the two prototypes was made using the visible-NIR spectrometer with a white light source transmitted through a NIR polarizer. The data is shown in Figure 13 where it can be seen that both prototypes are trending toward maximum reflectivity for S-Polarized illumination at 1064nm. (A better measurement with a NIR responsive spectrometer and a NIR polarizer was not possible at the time).

The ZnS coated sample, BZ19 (color code Tangerine on the results chart), fared poorly with total failure at a threshold of just under 1 J/cm². Prototype BT24 coated with Ta₂O₅ (color code Black on the results chart), fared much better showing no damage up to 3 J/cm², and a failure threshold of greater than 4 J/cm². This result is consistent with the prevailing industry knowledge that the softer, higher absorption ZnS material would exhibit lower damage thresholds. Based on information presented at the symposium outlining the development history of high damage threshold thin-film interference coatings, an SSR design based on hafnium oxide (HfO₂) as the high refractive index material deposited by e-beam evaporation may exhibit higher damage thresholds. Also promising is the concept of using thicker material layers in combination with one or two additional micro-structured layers in order to shift the maximum electric field intensity into the more durable material layer.

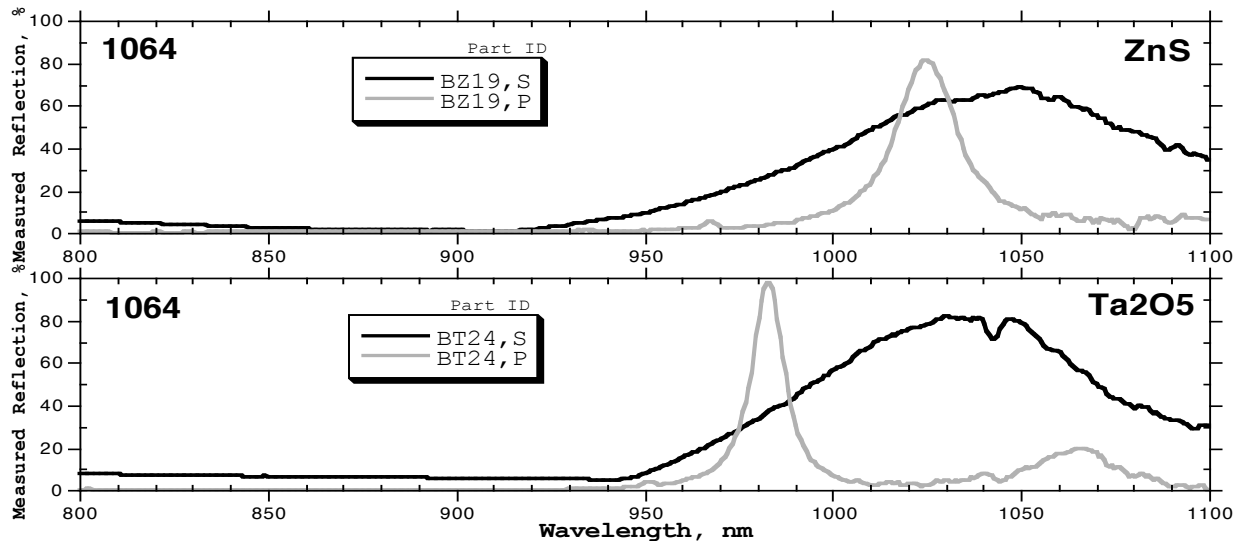


Figure 13: Measured reflection of the polarizing SSR mirrors submitted to the Damage Competition.

6.4 LIDT Testing at 1573nm

High power lasers operating at NIR wavelengths near 1550nm are common in optical telecommunications systems and in many military sensing and weapon systems. The pulsed laser damage thresholds for mirrors and optics at these wavelengths must be continually advanced to keep pace with the increasing power levels required. The simple design of SSR laser mirrors may provide a path toward higher damage thresholds. To evaluate the LIDT of SSR mirrors at 1550nm, multiple prototypes were fabricated on 1 and 2-inch diameter Schott Borofloat 33 glass windows. Half the prototypes were coated with ZnS by e-beam evaporation, and the other half were coated with Ta₂O₅ deposited by ion assisted deposition. The measured reflection of SSR mirror prototypes designed for 1538nm resonance is shown in Figure 14 along with cross sectional diagrams of the single layer design. (Again the back surface reflections are eliminated by fluid coupling to a high performance Random AR textured substrate during the measurement.) The top plot of Figure 14 shows three SSR samples coated with ZnS, and the bottom plot shows samples coated with Ta₂O₅. Due to multiple errors in the prototype fabrication process, most of the samples resonate at a longer wavelength than the 1538nm wavelength target. Fortunately, Quantel can configure their damage test for a wavelength of 1573nm to better match the resonant wavelength of the SSR prototypes. Note that only one sample, the ZnS coated prototype BZ57, exhibits a reflectivity that closely matches the model prediction, indicating that the microstructure fabrication process needs further development.

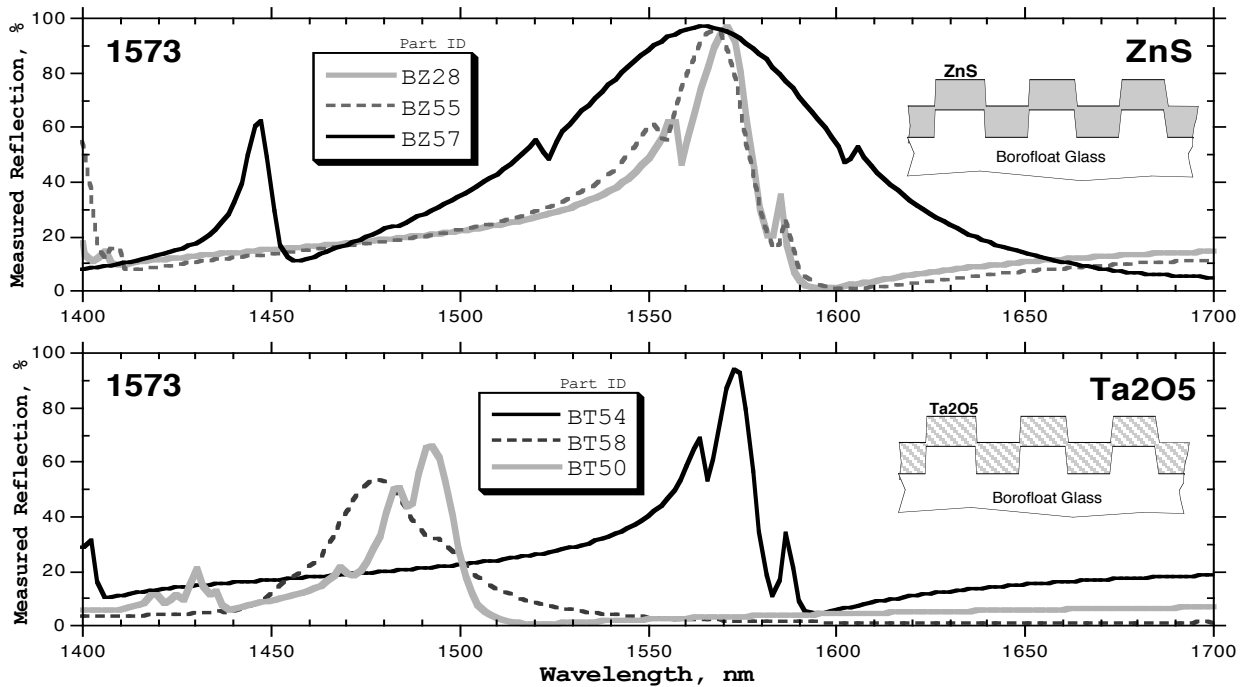


Figure 14: Measured reflection of non-polarizing SSR reflectors submitted for LIDT tests at 1573nm.

The results of the Quantel LIDT testing at 1573nm are shown in Figure 15. Only the four prototypes with reflection efficiencies above 90% near 1573nm were submitted for LIDT testing. Quantel exposed 90 locations on each window to 10 different fluence levels using a linearly polarized, pulsed laser with a 14ns pulse length and a 0.3mm spot size ($TEM_{00} - 1/e^2$). The pulse repetition rate was 20Hz allowing 200 pulses at each location. Again the damage criteria was a permanent surface change as observed by visual inspection through a microscope. The damage thresholds for the non-polarizing SSR mirrors coated with ZnS are 1.5 J/cm² for BZ28, 1.6 J/cm² for BZ55, and 3.0 J/cm² for BZ57. The Ta2O5 SSR mirror damage threshold is just 1.5 J/cm² for BT50. These results again appear low compared to the 15 J/cm² levels typically quoted by mirror vendors.

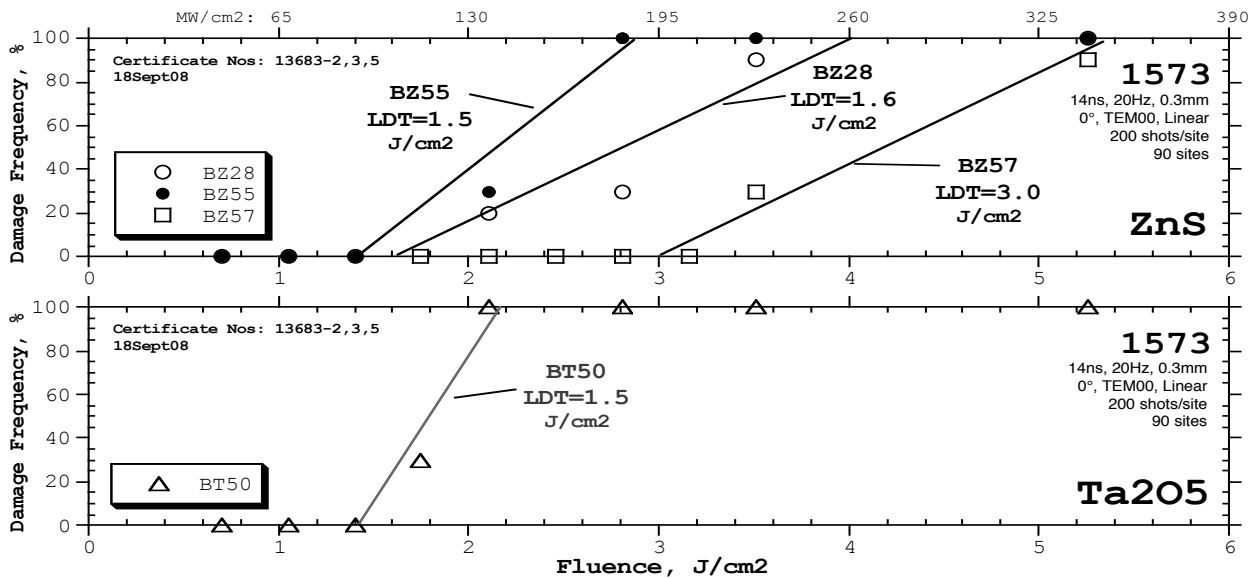


Figure 15: Results of 1573nm LIDT tests of SSR mirrors coated with ZnS (top) and Ta2O5 (bottom).

7. SUMMARY

Microstructure-based wavelength selective (referred to as surface structure resonators, SSR) mirrors have been fabricated in fused silica and Schott Borofloat 33 glass windows and tested for laser induced damage at three laser wavelengths ranging from the visible to NIR. Two waveguide material coatings deposited by different methods were evaluated. Pulsed laser damage thresholds were found to range from 0.5 to 4.0 J/cm², a level that is low relative to values found in the literature and reported by thin-film coating vendors. Figure 16 is a bar chart grouped by wavelength summarizing the SSR mirror damage threshold test results. Bars with the solid black band indicate a prototype tested at the resonant wavelength. Bars with diagonal slash marks indicate a prototype tested at a wavelength just slightly off the peak resonance, and bars with horizontal marks indicate a prototype tested at a wavelength far from the resonant wavelength. The results of this initial study vary significantly making it difficult to observe expected trends such as higher thresholds for the more dense and less absorbing Ta2O5 coating over the softer ZnS coating, and higher thresholds for microstructures etched in the more durable fused silica substrate material. The study results do however indicate that great improvements to the damage threshold of micro-structured reflectors are possible with further development using the concepts proven effective for high damage threshold multi-layer thin-film interference coatings.

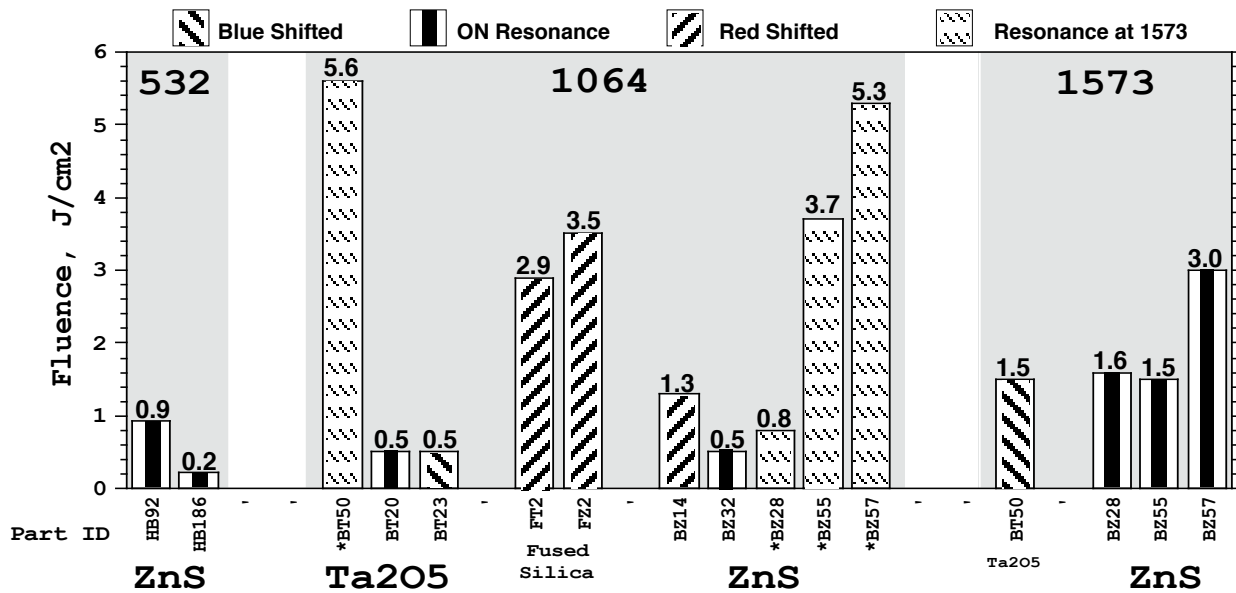


Figure 16: Summary of LIDT test results.

8. ACKNOWLEDGEMENTS

The authors wish to thank Jeff Runkel of Quantel USA (Big Sky Laser) who provided many helpful discussions and all of the certified, NIST traceable LIDT testing presented. Omega Optical of Vermont provided the ZnS and Ta2O5 coatings and some near infrared transmission data. Several dozen microstructure prototypes were fabricated with hard work from both Linda A. Palmaccio and Ernest Sabatino, III. SEM analysis was performed as a service by Mr. John Knowles at MicroVision Laboratories, Inc., (978-250-9909).

9. REFERENCES

- [1] MacLeod, H.A., [*Thin Film Optical Filters*, Third Edition], Institute of Physics Publishing, Bristol, , (2001)
- [2] Tayeb, G., Gralak, B., and Enoch, S., "Structural Colors in Nature and Butterfly-Wing Modeling", *Optics and Photonics News* Vol. 14, No.2, pg 38, (2003)
- [3] Cowan, J. J., "Aztec surface relief volume diffractive structure", *JOSA A* Vol. 7, No. 8, pg 1529, (1990)
- [4] Ghiradella, H., "Light and color on the wing: structural colors in butterflies and moths", *Applied Optics* 30, (1991)
- [5] Cowan, J. J., "Electro-Optic Device Allowing Wavelength Tuning", US Patent 6707518, (2004)
- [6] Cowan, J. J., "Advances in Holographic Replication with the Aztec Structure", *Proceedings of the International Conference on Holography, Wales, ,* (2006)
- [7] Raguin, D.H. and Morris, G.M., "Structured surfaces mimic coating performance", *Laser Focus World*, pg 113, (1997)
- [8] Mashev, L. and Popov, E., "Zero Order Anomaly of Dielectric Coated Gratings", *Optics Communications* Vol. 55, No. 6, pg. 377, (1985)
- [9] Mazuruk, K., "Bragg diffraction in the vicinity of Woods anomalies", *JOSA A* Vol. 7, No. 8, pg. 1464, (1990)
- [10] Wang, S.S., Magnusson, R., Bagby, J.S., and Moharam, M.G., "Guided-mode resonances in planar dielectric-layer diffraction gratings", *JOSA A* Vol. 7., No. 8, pg. 1470, (1990)
- [11] Magnusson, R., and Wang, S.S., "New principle for optical filters", *Appl.Phys.Lett.*, 61(9), pg.1022, 1992
- [12] Wang, S. S., and Magnusson, R. "Theory and applications of guided-mode resonance filters", *Applied Optics* Vol. 32, No. 14, pg 2606, (1993)
- [13] Wang, S. S., and Magnusson, R. "Design of waveguide-grating filters with symmetrical line shapes and low sidebands", *Optics Letters* Vol. 19, No. 12, pg 919, (1994)
- [14] Peng, S. and Morris, M., "Experimental demonstration of resonant anomalies in diffraction from two-dimensional gratings", *Optics Letters*, Vol. 21, No. 8, pg 549, (1996)
- [15] Peng, S. and Morris, M., "Resonant Scattering from two-dimensional gratings", *JOSA A* Vol. 13, No. 5, pg. 993, (1996)
- [16] Sharon, A., et. al. "Resonant grating-waveguide structures for visible and near infrared radiation", *JOSA A* Vol. 14, No. 11, pg. 2985, (1997)
- [17] Brundrett, D., et. al., "Normal-incidence guided-mode resonant grating filters: design and experimental demonstration", *Optics Letters*, Vol. 23, No. 9, pg.700, (1998)
- [18] Tibuleac, S., and Magnusson, R., "Reflection and Transmission Guided-mode Resonance Filters", *JOSA A* Vol. 14, No. 7, pg 1617, (1997)
- [19] Priambodo, P.S., Maldonado, T.A., and Magnusson, R., "Fabrication and Characterization of High-Quality Waveguide-mode Resonant Optical Filters", *Applied Physics Letters* Vol. 83(16), pg 3248, (2003)
- [20] Magnusson, R., and Wang, S.S., "Transmission band-pass guided-mode resonance filters", *Applied Optics* Vol. 34, pg 8106, (1995)
- [21] Magnusson, R., et.al., "Efficient Band-pass Reflection and Transmission Filters With Low Sidebands Based on Guided-Mode Resonance Effects", US Patent 5598300, (1997)
- [22] Hobbs, D.S. and Cowan, J. J., "Optical Device For Filtering and Sensing", US Patent 6791757, (2004)
- [23] Hobbs, D.S., "Laser-Line Rejection or Transmission Filters Based on Surface Structures Built on Infrared Transmitting Materials", *Proc. SPIE* Vol. 5786, (2005)
- [24] Hobbs, D.S., et. al., "Automated Interference Lithography Systems for Generation of Sub-Micron Feature Size Patterns", *Proc. SPIE* Vol. 3879, pg 124, (1999)